

Human umbilical cord mesenchymal stem cells contribute to the reconstruction of bladder function after acute spinal cord injury via p38 mitogen-activated protein kinase/nuclear factor-kappa B pathway

Jue Li^{1,2}, Jiliang Huang³, Ling Chen¹, Wei Ren¹, and Wenzhi Cai ^{1,2}

¹Department of Nursing, Shenzhen Hospital, Southern Medical University, Shenzhen, Guangdong, 518101, P.R. China; ²School of Nursing, Southern Medical University, Guangzhou, Guangdong, 510515, P.R. China; ³Reproductive Center, The First Affiliated Hospital of Shantou University Medical College, Shantou, Guangzhou, Guangdong, 515041, P.R. China

ABSTRACT

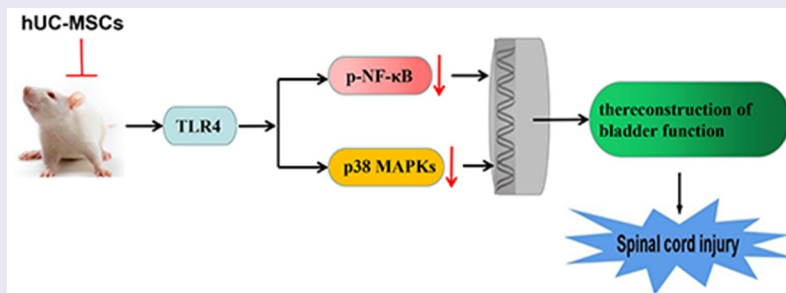
The association between spinal cord injury (SCI) and bladder symptoms has been intensively described. Human umbilical cord mesenchymal stem cell (hUC-MSC) treatment is beneficial to the recovery of bladder function after SCI, but its mechanism is unclear. We established an SCI model, and prepared hUC-MSCs in advance, followed by verification using flow cytometry. The Basso, Beattie and Bresnahan (BBB) score and urodynamic index were employed to evaluate motor function and bladder functions, respectively. Hematoxylin–eosin staining, luxol fast blue staining, and Masson's trichrome staining were utilized to assess pathological changes. Real-time quantitative PCR and Western blot were used to determine the mRNA and protein expressions in bladder tissues. The immunophenotypes of the hUC-MSCs were CD90⁺ and CD105⁺, but CD34⁻, CD45⁻ and HLA-DR⁻. Rats appeared severe motor dysfunction after SCI, but the BBB score was increased in hUC-MSCs after the second week. Pathologically, the improvement of the lesion area on the dorsal spinal cord, augmented anterior gray horn neuron cells of the spinal cord and lessened bladder tissue remodeling (fibrosis, collagen deposition) as well as modulated inflammation could be observed. Besides, SCI increased bladder weight, bladder capacity, urine volume and residual urine volume, and decreased urination efficiency. HUC-MSCs ameliorated SCI-induced pathological changes and bladder functions, the expressions of Collagen I, Collagen III, fibroblast growth factor 2 (FGF2), phospho-p38, transient receptor potential vanilloid 1, Toll-like receptor 4 and phospho-nuclear factor-kappa B (p-NF-κB). To sum up, HUC-MSCs contribute to the reconstruction of bladder function after SCI by repressing p38 MAPK/NF-κB pathway.

ARTICLE HISTORY

Received 16 August 2021
Revised 24 January 2022
Accepted 25 January 2022

KEYWORDS

Spinal cord injury; human umbilical cord mesenchymal stem cells; bladder function; p38 MAPK/NF-κB signaling pathway






Introduction

Spinal cord injury (SCI) is a traumatic central nervous system disease with a high disability rate, leading to varying degrees of motor, sensory and sphincter dysfunction [1,2]. The global incidence of SCI is 10.4–83 cases per 1,000,000 population, which is still on the rise [3]. Despite decades of

research on SCI, the therapeutic effects and results on patients suffering from this disease fall short of expectation.

The progression of acute SCI consists of two phases, namely, primary and secondary injuries. Due to the impaired link between the brain and

CONTACT Wenzhi Cai  caiwzh@smu.edu.cn  Department of Nursing, Shenzhen Hospital, Southern Medical University No. 1333 Xinhua Road, Baoan, Shenzhen, Guangdong, 518110, China

 Supplemental data for this article can be accessed [here](#)

© 2022 The Author(s). Published by Informa UK Limited, trading as Taylor & Francis Group.

This is an Open Access article distributed under the terms of the Creative Commons Attribution-NonCommercial License (<http://creativecommons.org/licenses/by-nc/4.0/>), which permits unrestricted non-commercial use, distribution, and reproduction in any medium, provided the original work is properly cited.

the peripheral nervous system, SCI can cause a range of comorbidities, such as neurogenic bowel, neurogenic bladder and sexual dysfunction [4–6]. Neurogenic bladder, one of the culprits that undermine the life quality of patients with SCI, can be described as an altered micturition reflex in pathophysiology, leading to the increment in compliance, volume and residual volume of bladder, and continuous leakage of urine [6,7]. Modern treatments mainly address the physiology of neurogenic bladder at the bladder level rather than the neurologic trauma, such as catheterization, oral medication and surgery (bladder enlargement or urinary diversion) [8,9]. Encouragingly, with advances in cell culture technology and developmental biology, cell therapy and tissue engineering technology have made huge strides in the neuroprotection and nerve regeneration against SCI, with clinical trials being actively under way [10–12].

Mesenchymal stem cells (MSCs) are pluripotent stromal cells derived from bone marrow, adipose tissue, umbilical cord, etc., with strong self-renewal ability and multilineage potential [11,13]. MSCs are excellent candidates for cell therapy, especially human umbilical cord-MSCs (hUC-MSCs), which are exceedingly prevailing in regenerative medicine thanks to their easy access, faster self-renewal capacity, low immunogenicity, and minimal ethical issues [14]. Xiao et al. pointed out that the recovery of sensory (such as bowel and bladder) and motor functions of two patients with acute SCI, who had been diagnosed with complete injury, were observed 1 year after receiving NeuroRegen scaffolds with hUC-MSCs transplanted into the injury site [15]. The transplantation of hUC-MSCs is considerable for the recovery of bladder function after SCI [14–16]. However, as far as we know, the mechanisms involved are rarely investigated.

Most patterns of SCI in humans can be replicated in rats, which have become the primary model for evaluating therapeutic strategies and understanding the pathological basis of SCI [2,17,18]. Herein, we hypothesized that hUC-MSCs have a positive function in improving SCI. In this study, a rat model of acute SCI-induced neurogenic bladder was constructed *in vivo*, and hUC-MSCs were isolated to dig deep into the

mechanism in acute SCI-induced neurogenic bladder, with the expectation to offer a foundation for the application of stem cells in the treatment of SCI-induced bladder dysfunction.

Materials and methods

Preparation of hUC-MSCs

The implementation of the study was approved by the Ethics Committee of Shenzhen Hospital of Southern Medical University (XSE202004250511). Three fresh umbilical cord samples from healthy newborn fetuses delivered in our hospital were collected for the preparation of hUC-MSCs, with the written informed consent of their mothers. Aseptically, the blood vessels and the outer membrane of the umbilical cord were removed, followed by being washed with phosphate-buffered saline (PBS; $1 \times$ PBS, pH = 7.2, 806544, Merck, USA). Then, the remaining lumen was cut into small pieces of about $1\text{--}2\text{ mm}^3$ and cultured in Dulbecco's Modified Eagle's Medium (DMEM, 30–2002, American Type Culture Collection (ATCC), USA) containing 10% fetal bovine serum (FBS, 16140071, Thermo Fisher, USA), platelet-derived growth factor ($10\text{ }\mu\text{g/L}$, P5208, Merck, USA), basic fibroblast growth factor ($10\text{ }\mu\text{g/L}$, HEGFP-0602, Cyage (Suzhou) Biotechnology Co., Ltd., Suzhou, China) and penicillin (100 U/mL)-streptomycin ($100\text{ }\mu\text{g/mL}$) solution (30–2300, ATCC, USA) in an incubator at 37°C with 5% CO_2 (Herocell 180, Radobio Scientific Co., Ltd., Shanghai, China). The medium was changed every 3 days. One week later, non-adherent cells were removed using PBS, and the remaining adherent cells were defined as primary cells for passage.

hUC-MSC marker detection

The hUC-MSCs at second passage (P2) were made into a single-cell suspension (3×10^6 cells/mL) with complete medium. The antibodies used were purchased from BD Pharmingen. HUC-MSCs were characterized by being labeled with antibodies against cluster of differentiation (CD) CD34-FITC (555821) and CD45-FITC (555482), and the human leukocyte antigen-DR markers (HLA-DR)-

FITC (556643), CD90-FITC (555595) and CD105-FITC (561443). The antibody-bearing cells were incubated at 4°C for 30 minutes (min), and then fixed with 4% paraformaldehyde (PFA, P804536, Maclin, Shanghai, China). The expressions of markers were detected by Accuri C6 Plus Flow Cytometer (BD Pharmingen, USA). The P3 hUC-MSCs were used in the follow-up experiments.

SCI animal model and therapeutic measures

The animal experiment was approved by the Ethics Committee of Shenzhen Hospital of Southern Medical University (R20200522) and carried out in accordance with the guidelines for the care and use of experimental animals. Twenty-four 13-week-old female Sprague Dawley rats (250–300 g, SPF-004, <http://www.lasmark.cn>, Beijing, China) were bred in a specific pathogen-free (SPF) grade room with humidity of 50–70%, 12-h light–dark cycle, temperature of 24–26°C and given free access to food and water. The 24 rats were randomly and equally divided into four groups: control group ($N = 6$), sham group ($N = 6$), model group ($N = 6$), and hUC-MSCs group ($N = 6$). In the control group, rats were kept normally without any treatment. In the model group (SCI group), rats were anesthetized with Zoletil-50 (Zoletil®50, Virbac, France) (intraperitoneal injection, 1 mg/kg), and then laminectomy was performed at the T8/T9 vertebrae that was identified by counting from the last rib level to cranium. The multiple dorsal processes at vertebrae T8/T9 were transected with microscissors to induce SCI [18,19]. After the trauma, the rats were subcutaneously administered with buprenorphine (0.05 mg/kg, B7536, Merck, USA) and gentamicin (8 mg/kg, L1312, Solarbio, Beijing, China) for three consecutive days. Besides, additional abdominal compression was conducted on SCI rats to empty their bladder (twice a day) until normal urinary tract reflexes were observed. On the eighth day, PBS solution (P903593, Macklin, Shanghai, China) was injected into the spinal cord with a Hamilton needle (Beijing Braun Science and Technology Co., Ltd., Beijing, China). In the Sham group, rats underwent the same operation without

spinal cord damage and were then injected with the same amount of PBS. In the hUC-MSCs group, rats were induced SCI through surgery, and received postoperative care. 0.25% Trypsin-EDTA (C0201, Beyotime, Beijing, China) was used to prepare the suspension of hUC-MSCs. On the eighth day after the induction of SCI, approximately 6×10^5 hUC-MSCs were injected into the spinal cord with the Hamilton needle [20]. None of the animals utilized became ill or died prior to the experimental endpoint.

The Basso, Beattie and Bresnahan (BBB) score

BBB rating scale was used to evaluate motor function of rats after surgery. On the first day before SCI, all the rats involved were raised in an open environment for BBB behavior scoring once a week for a total of 8 weeks until the end of the test. This standard evaluation included parameters such as hind limb joint movement, paw placement, weight support, and forelimb-hind limb coordination, with 0 indicating no hind limb movement and 21 indicating normal rat movement [21,22].

Bladder function assessment

Before sacrifice, the rats were evaluated for urodynamics on the premise of consciousness. Each rat was placed in a metabolic cage (Lab products, USA) alone. Under the anesthesia using Zoletil-50, the bladder was emptied and catheterized (PE50, Smith Medical, UK). A small incision was made in the bladder and sutured with non-absorbable monofilament suture for purse-string suture (6-0, Riverlon, Medical EXPO, USA). Then, two PE50 tubes were preheated to form a collar and tightly implanted into the bladder dome. One tube was connected to an infusion pump (Legato100, KD Scientific, USA), and the other was connected to a pressure sensor (ML866 PowerLab, ADI Instruments, Australia). Then, 0.9% saline was infused into the bladder at a steady rate (0.1 mL/min). Bladder weight, bladder capacity, urine volume, residual urine volume and urination efficiency were recorded for evaluation of bladder functions.

Sample collection

The rats were euthanized by intraperitoneal injection with an overdose of pentobarbital solution (130 mg/kg, P-010-1ML, Merck, USA). The injured spinal cord tissues (about 1 cm in length) and bladder tissues were separated. The bladder weight was measured, and the value was expressed as an average value. Besides, some bladder tissues were taken for the extraction of RNA and protein and stored at -80°C . Then, the collected tissues were fixed with 4% paraformaldehyde (P885233, Macklin, Shanghai, China) and made into paraffin-embedded samples according to the procedures (ASP300S, Leica, Germany). Finally, the tissues were crosscut into a series of sections with a thickness of 6 μm (LS-2065, Shenzhen Dakway Medical Technology Co., Ltd., Shenzhen, China) for histological analysis.

In addition, part of the bladder tissues was treated with Trizol solution (15596026, Thermo Fisher, USA) and phenol-chloroform (288306, P1037, Merck, USA) to extract total RNA. Then, reverse transcription kit (RR036Q, TaKaRa, Japan) was used to synthesize cDNA efficiently. Another part of the bladder tissues was thoroughly ground and treated with the RIPA Lysis buffer (89901, Thermo Fisher, USA) to extract total proteins. The final samples were stored at -80°C .

Immunofluorescence

Eight weeks post transplantation, we estimated the survival rate of hUC-MSCs transplanted into the injured spinal cords. Paraffin sections were dewaxed and rehydrated, and then repaired with antigen. After being blocked, the sections were exposed to primary antibody against human nuclear (HuNu; 1:500, ab216943, Abcam, UK) at 4°C overnight, followed by reaction with secondary antibody goat anti-mouse IgG H&L (Alexa Fluor[®] 594, ab150120, Abcam, UK). Next, the nuclei were counterstained with DAPI Staining Solution (ab228549, Abcam, UK). The model group functioned as the negative control group. After the sections were mounted with the glycerol jelly mounting medium (S2150,

Solarbio, China), the immunofluorescent images were acquired using a fluorescence microscope (BX53, OLYMPUS, Japan).

Histological staining

Hematoxylin–eosin staining (HE)

Deparaffinized sections were stained with HE staining kit (C0105S, Beyotime, Shanghai, China). According to the instructions, the sections were subjected to xylene dewaxing and gradient ethanol hydration. Then, hematoxylin staining solution was applied to stain the sections for 3 min. After being rinsed with tap water for 10 min, eosin staining was taken to treat the sections for 45 seconds (s). Following dehydration and transparency, Glycerol Jelly Mounting Medium was employed to seal the sections. Finally, the pathological abnormalities were observed and photographed under an inverted microscope (IXplore Pro, OLYMPUS, Japan).

Luxol Fast Blue (LFB) staining

Deparaffinized sections were stained with LFB myelin staining solution (G3240, Solarbio, Beijing, China). As per the instructions, the sections were immersed in LFB staining solution at room temperature overnight. On the next day, 95% ethanol (E801077, Macklin, Shanghai, China) was used to remove the excess staining solution. Then, the sections were differentiated in luxol differentiation solution for 15 s, followed by being submerged in 70% ethanol for 30 s until the gray matter was clear. Ultimately, the eosin staining solution was used to counterstain the sections for 1 min. Eventually, the results of staining were observed, and the photos of the sections were taken.

Masson's trichrome staining

Deparaffinized sections were stained with Masson's trichrome staining kit (G1340, Solarbio, Beijing, China). In line with the instructions, the sections were stained with Weigert's iron

hematoxylin working solution for 10 min and differentiated in acidic ethanol differentiation solution for 15 s, followed by being immersed in Masson's blue liquid for 4 min. Then, the sections were further stained with ponceau red fuchsin staining solution for 6 min and aniline blue staining solution for 2 min. Finally, the staining results were observed and the images of the sections were photographed.

Real-time quantitative PCR (q-PCR)

Prepared cDNA was functioned as a template. Next, q-PCR was performed on ABI 7300 instrument (Applied Biosystems, USA) and its parameters were set as follows: 95°C for 30 s, followed by 95°C for 5 s, and 60°C for 30 s with 38 cycles. GAPDH was proposed as the internal control. Relative quantification method $2^{-\Delta\Delta C_t}$ was utilized to represent the relative expression. The primers involving genes were appended in Table 1.

Western blot

Total proteins were quantified using BCA protein assay kit (23225, Thermo Fisher Scientific, USA), then mixed with protein loading buffer (C516031, Sangon Biotech, Shanghai, China) and denatured at 95°C. The proteins were separated by sodium dodecyl sulfate-polyacrylamide gel electrophoresis (SDS-PAGE) (Bio-Rad, USA) and transferred onto polyvinylidene difluoride membrane (3010040001, Merck, USA) for 120 min at 40 V and 120 mA. Nonspecific binding sites on the membrane were blocked with 5% fat-free milk at room temperature for 2 h. Next, primary antibodies against Collagen I (ab270993, Abcam, UK, 139 kDa, 1:1000), Collagen III (ab7778, Abcam, UK, 138 kDa, 1:5000), fibroblast growth factor-2 (FGF 2) (ab171941, Abcam, UK, 22 kDa, 1:1000), p-p38 (ab47363, Abcam, UK, 41 kDa, 1:1000), P38

(ab170099, Abcam, UK, 42 kDa, 1:1000), transient receptor potential vallinoid 1 (TRPV1) (ab203103, Abcam, UK, 95 kDa, 1:1000), toll-like receptor 4 (TLR4) (ab13867, Abcam, UK, 90 kDa, 1:500), NF- κ B (#8242, cell signaling technology (CST), USA, 65 kDa, 1:1000), p-NF- κ B (#3039, CST, 65 kDa, 1:1000) and GAPDH (ab8242, Abcam, UK, 36 kDa, 1:1000) were added to incubate the membrane at 4°C overnight. GAPDH was served as the internal control. On the next day, the membrane was further incubated with horseradish peroxidase (HRP)-conjugated secondary antibodies Goat Anti-Rabbit IgG H&L (ab205718, Abcam, UK, 1:50,000) and Goat Anti-Rabbit IgG (ab205719, Abcam, UK, 1:10,000) at room temperature for 2 h. Finally, the protein strips (Bio-Rad ChemiDoc Touch, Bio-Rad, USA) were visualized using a chemiluminescence kit (BeyoECL Plus, P0018S, Beyotime, Shanghai, China).

Statistical analysis

The measurement data were described as the mean \pm standard deviation, and the comparison among multiple groups was performed by one-way analysis of variance (ANOVA). All statistical analyses were implemented by GraphPad Prism 8.0 software (GraphPad Software, USA). Statistical significance was indicated by $P < 0.05$.

Results

The association between SCI and bladder symptoms has been widely acknowledged, and hUC-MSC treatment is manifested to be beneficial to the recovery of bladder function after SCI, but its specific molecular mechanism is still missing. We hypothesized that hUC-MSCs have positive functions in ameliorating SCI. A rat model of acute SCI-induced neurogenic bladder was constructed *in vivo* and hUC-MSCs were isolated to probe into

Table 1. List of q-PCR primers used in this study.

Gene (Human)	Forward primer (5'→3')	Reverse primer (5'→3')
<i>Collagen I</i>	CCAGCCGCAAAGAGTCTACATGTC	TCACCTTCTCATCCCTCCTAA
<i>Collagen III</i>	CGGAGGAATGGGTGGCTATC	ACCAGCTGGGCCTTTGATAC
<i>FGF 2</i>	AGTGCCTTACACAATGGTTC	ACCACGCTTCTTCTGACATCG
<i>TRPV1</i>	GAATGACACCATCGCTCTGC	AAGAGGGTCACCAGCGTCAT
<i>TLR4</i>	TGGCATCATCTTCATTGTCC	CAGAGCATTGTCTCCCACT
<i>GAPDH</i>	GATGAACCTAAGCTGGGACCC	TGTGAACGGATTGGCCGTA

the underlying mechanism in acute SCI-induced neurogenic bladder. We discovered that hUC-MSCs contributed to the reconstruction of bladder function after SCI by repressing p38 MAPK/NF- κ B pathway.

Cultivation and identification of hUC-MSCs

The primary hUC-MSCs were successfully isolated by explant culture methods. Heaps of spindle-shaped cells could be observed in P2 hUC-MSCs, which resembled fibroblast in appearance (Figure 1(a)). Flow cytometry was used to detect specific antigen markers on the surface of P2 hUC-MSCs. Among them, CD105 is a marker of mesenchymal stem cells, CD90 is a mesenchymal-related antigen, and CD34 and CD45 are positive markers of hematopoietic

stem cells [23]. Moreover, HLA-DR is a human major histocompatibility complex (MHC) antigen. The immunophenotypes of hUC-MSCs were CD90⁺ >97% and CD105⁺ >97%, CD34⁻, CD45⁻ and HLA-DR-negative, signifying that the surface-specific antigen markers of hUC-MSCs were consistent with those of the MSCs in bone marrow, cord blood and other tissues (Figure 1(b)). Additionally, the lack of HLA-DR expression indicated weak immunogenicity (Figure 1(b)).

Transplantation of hUC-MSCs partially restored the motor function of SCI rats by ameliorating the destructive lesions

Rats undergoing SCI model surgery developed severe hindlimb dyskinesia since the first day.

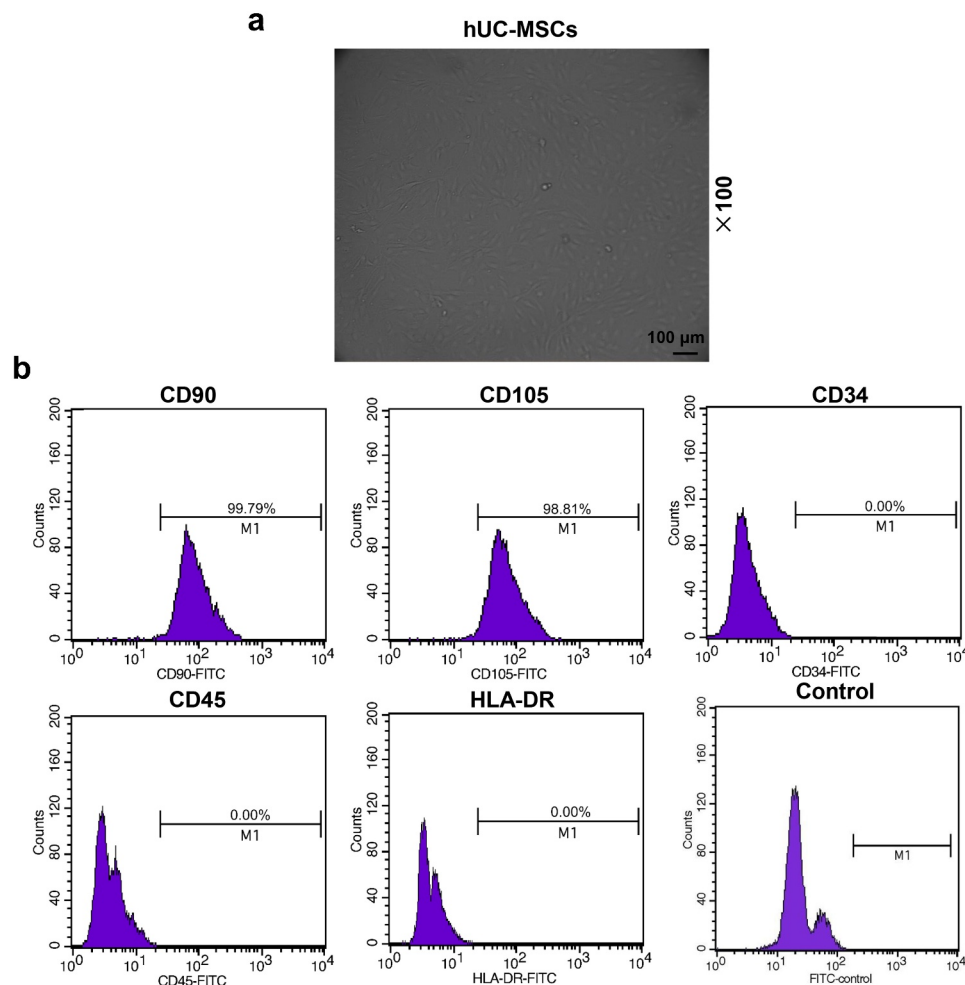


Figure 1. Cell culture and identification of human umbilical cord mesenchymal stem cells (hUC-MSCs). (a) Representative image of isolated P2 hUC-MSCs. A large number of spindle cells that resemble fibroblasts were observed (scale: 100 μm; magnification: 100 ×). (b) Flow cytometry was used to detect the surface markers of hUC-MSCs like clusters of differentiation (CD) (CD90, CD105, CD34, CD45), and human leukocyte antigen-DR markers (HLA-DR) .

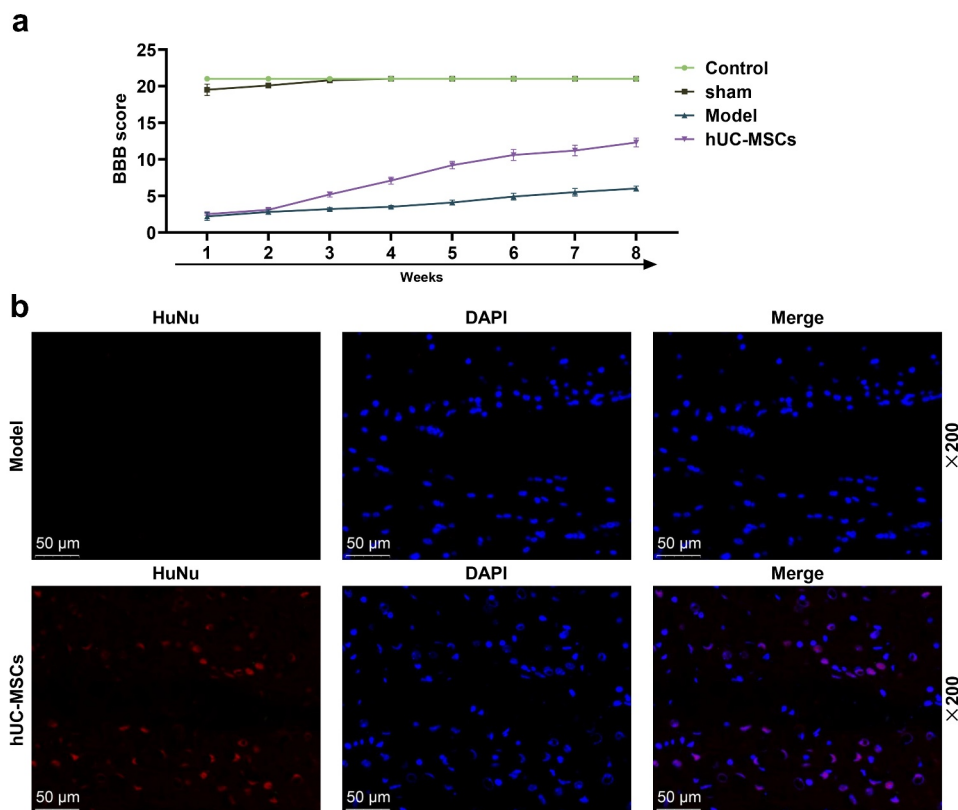


Figure 2. Transplantation of hUC-MSCs continued to survive in the spinal cord after 8 weeks. (a) The Basso, Beattie and Bresnahan (BBB) score was used to assess the motor function of Control, Sham, SCI or hUC-MSCs group rats from the first week to the eighth week of modeling. HUC-MSCs helped SCI rats recover their exercise capacity. (b) The immunofluorescence staining exhibited that transplanted hUC-MSCs continued to survive in the spinal cord after 8 weeks (scale: 50 μm; magnification: 200×).

After the second week, the BBB score in the hUC-MSCs group was clearly improved in comparison with that in the model group (Figure 2(a)). Next, immunofluorescence staining exhibited that transplanted hUC-MSCs continued to survive in the spinal cord after 8 weeks. As illustrated in Figure 2(b), in the hUC-MSCs group, we could observe the surviving transplanted hUC-MSCs in the spinal cord. In contrast, no transplanted hUC-MSCs were discovered in the model group (negative control group).

Afterward, we pathologically analyzed the spinal cord tissues, neuronal cells, and bladder tissues of the rats to explore the healing effect. SCI resulted in necrosis of the rat spinal cord dorsal tissue, accompanied by cell debris and inflammatory cell infiltration (Figure 3(a)), and toluidine blue staining demonstrated that the survival rate of pre-medullary gray horn neurons was dwindled (Figure 3(b-c), $P < 0.001$). After the injection of hUC-MSCs, spinal cord tissue lesions were ameliorated and the survival

rate of neuronal cells in rats was elevated (Figure 3(a-c), $P < 0.05$). In addition, inflammatory cell infiltration, vacuole-like structure, edema, vascular structure destruction, fibrosis, collagen deposition, and epithelial cell disorder could be observed in the SCI-modeled rat bladder tissues, while the degree of damage after hUC-MSCs treatment was decreased. Namely, the submucosal edema and bleeding marks, inflammatory cell infiltration, fibrosis, and collagen deposition were notably relieved (Figure 3(d-e)). The results above revealed that hUC-MSCs could alleviate destructive lesions in rats with SCI, the mechanisms of which were likely associated with impaired blood circulation, tissue nutrition and bladder function.

Effects of hUC-MSCs treatment on SCI-induced bladder dysfunction and related molecular mechanisms

SCI induced bladder dysfunction. Compared with rats receiving sham operation, the bladder capacity

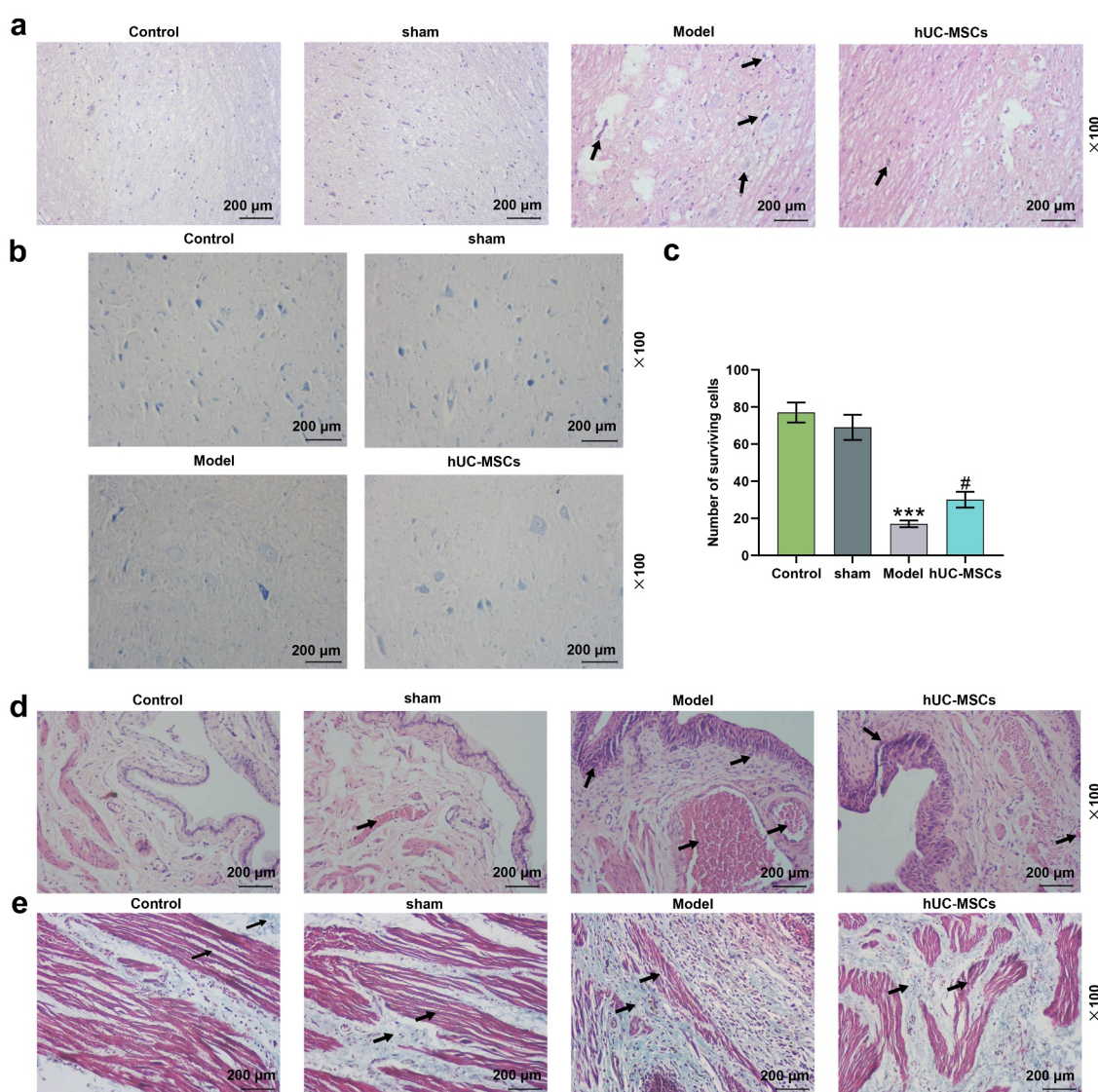


Figure 3. Transplantation of hUC-MSCs partially restored the motor function of spinal cord injury (SCI) rats by ameliorating the destructive lesions. (a–e) Transplantation of hUC-MSCs ameliorated spinal cord and bladder lesions induced by SCI. Hematoxylin–eosin (HE) staining of the dorsal side of the spinal cord (scale: 200 μ m; magnification: 100 \times) (a). Luxol fast blue (LFB) was applied to assess the survival rate of neuronal cells in the spinal cord injury area (scale: 200 μ m, magnification: 100 \times) (b–c). HE staining of bladder tissues (scale: 200 μ m; magnification: 100 \times) (d). Masson’s trichrome staining of bladder tissues (scale: 200 μ m; magnification: 100 \times) (e). *** $P < 0.001$ vs. Sham, # $P < 0.05$ vs. Model.

and urination volume of SCI modeled rats were elevated, with especially higher residual urine volume and urination efficiency (Figure 4(a–d), $P < 0.001$), whilst transplantation of hUC-MSCs alleviated SCI-induced increased bladder capacity, residual urine output and urinary output, thereby improving the efficiency of urination (Figure 4(a–d), $P < 0.05$). In addition, hUC-MSCs reduced SCI-induced gain of bladder weight (Figure 4(e), $P < 0.05$).

To investigate which molecules derived from hUC-MSCs participated in SCI-induced bladder dysfunction, we conducted q-PCR and Western blot. The mRNA and protein expressions of Collagen I, Collagen III and FGF were highly upregulated in the model group in comparison with those in the sham group, while these upregulated tendencies were mitigated by transplantation of hUC-MSCs (Figure 5(a–c), $P < 0.001$). Simultaneously, SCI promoted the expression

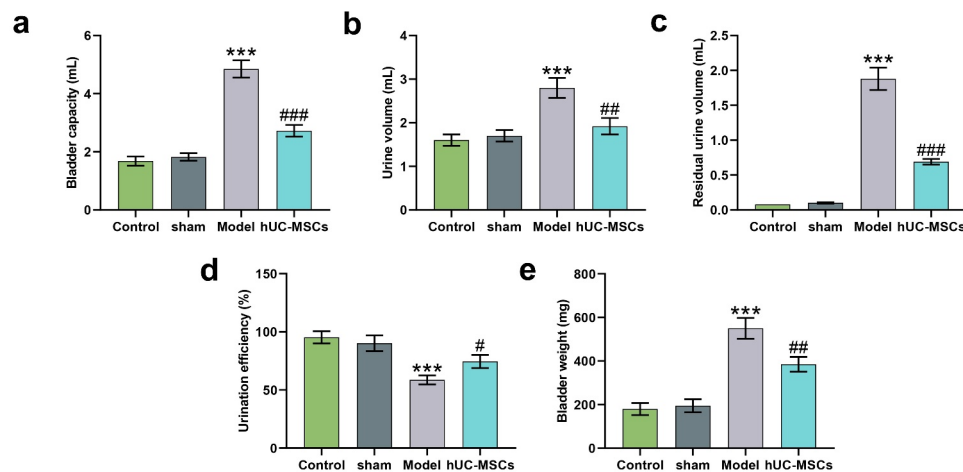


Figure 4. Transplantation of hUC-MSCs ameliorated bladder dysfunction induced by SCI. (a–d) Analyses of bladder functions, including bladder capacity (mL) (a), urine volume (mL) (b), residual urine volume (mL) (c) and urination efficiency (%) (d). (e) After the bladder examination, the bladder was taken for weight assessment (mg). *** $P < 0.001$ vs. Sham, # $P < 0.05$, ## $P < 0.01$, ### $P < 0.001$ vs. Model.

levels of p-p38, TRPV1, TLR4 and p-NF- κ B, which could also be reversed by hUC-MSCs (Figure 5(d–l), $P < 0.01$).

Discussion

The poor prognosis of patients with SCI is attributed to the extremely weak regenerative ability of the spinal cord, which is further complicated by pathological cascades of multiple interactions [24]. Cell transplantation is currently considered to be an unquestionably attractive and advancing field, which, in fact, has already bore fruits [25]. HUC-MSCs, as a type of new seed cells for the treatment of SCI, support revascularization, inflammation relief and microenvironment improvement. In murine and canine models, hUC-MSCs have been observed to improve post-SCI injury [26–28], which is feasible in markedly ameliorating muscle spasm, autonomic nervous system, as well as bladder and intestinal function [29]. Early interventions for SCI are critical to improve long-term results. In this study, we probed into the mechanism of hUC-MSCs on neurogenic bladder function after direct injection into the lesion in the early stage of SCI.

Axonal degeneration, death of oligodendrocytes and neurons, and scar formation caused by trauma ultimately lead to impaired neuronal function [13]. The improvement of motor and sensory functions

is considered to be the main criterion for evaluating therapeutical efficacy in SCI patients. The BBB test is recognized worldwide as the most practicable method in assessing the motor function of SCI rats [21]. After the transplantation of hUC-MSCs, the exercise ability of rats was partially restored, as suggested by the ameliorating effects of hUC-MSCs on inflammation of the spinal cord and survival rate of neuronal cells in the injury area.

The reconstruction of the patient's bladder function is an overriding priority in clinical practice. The normal detrusor allows the bladder to fill during the storage phase, with little or no change in bladder pressure [30]. In contrast, the neurogenic bladder can cause unconscious contraction of the detrusor and an increase in bladder pressure and contraction time [31]. Consistent with previous studies, our results evidenced that SCI-induced neurogenic cystitis sparked off augmented bladder volume, urine output, and especially residual urine volume, and decreased urination efficiency in rats. This series of complex reactions covered tissue remodeling and inflammation, leading to bladder hypertrophy and fibrosis. The hypertrophy of the bladder and increased collagen deposition together impair the contractile properties of the bladder [32]. At the molecular level, we also confirmed that the model group expressed high mRNA and protein levels of Collagen I (2.67-

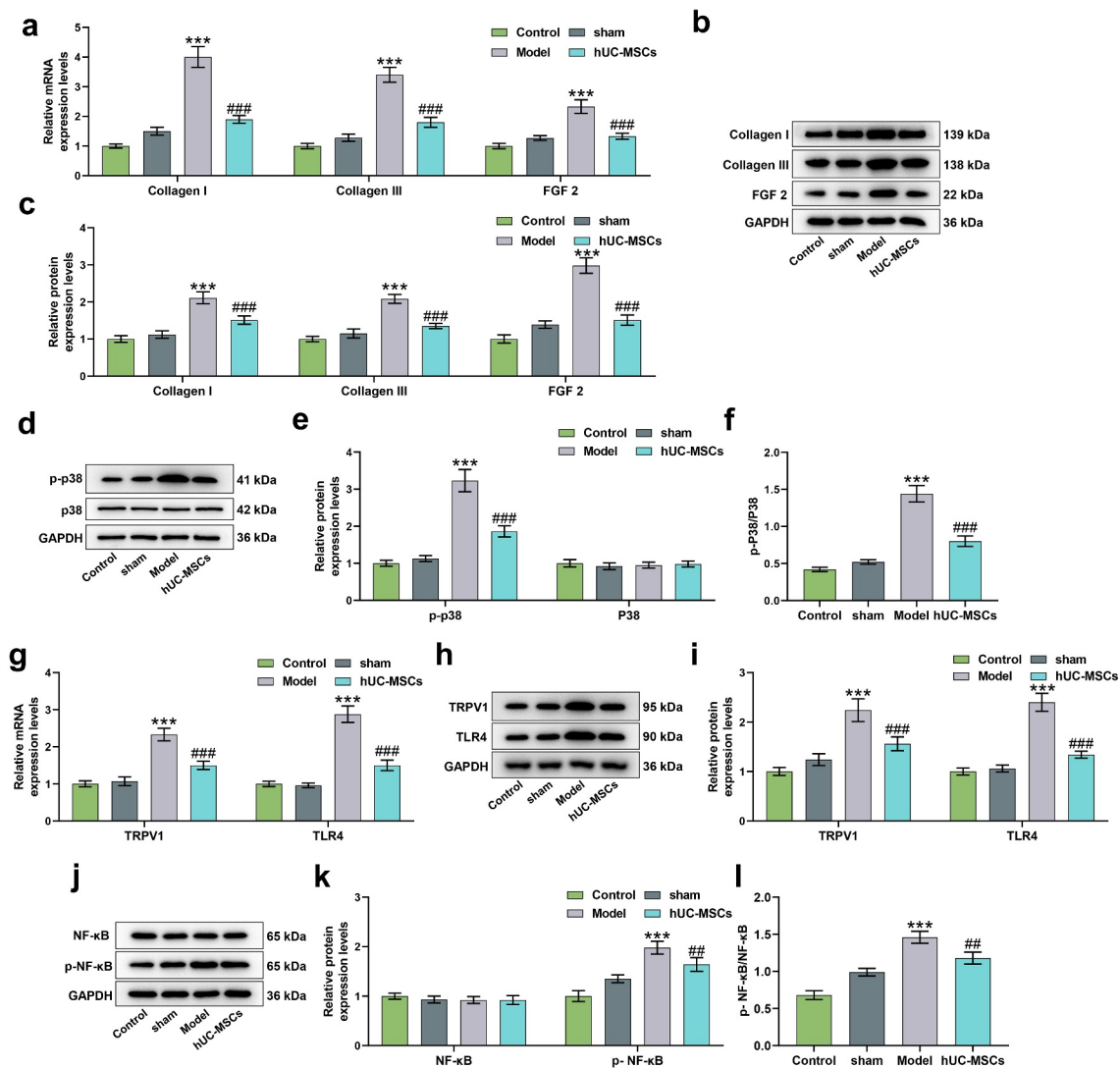


Figure 5. Real-time quantitative PCR (q-PCR) and Western blot were used to detect bladder tissue-related mRNA and protein expressions, respectively. (a–l) HUC-MSC treatment reversed the upregulations of Collagen I, Collagen III, fibroblast growth factor-2 (FGF 2) (a–c), p-p38 (d–f), transient receptor potential vallinoid 1 (TRPV1), toll-like receptor 4 (TLR4) (g–i) and p-NF-κB (j–l) induced by SCI. GAPDH was used as an internal reference. *** $P < 0.001$ vs. Sham, ## $P < 0.01$, ### $P < 0.001$ vs. Model.

fold and 1.91-fold), Collagen III (2.62-fold and 1.91-fold) and FGF 2 (1.77-fold and 2.14-fold) in bladder tissues than those of the sham group, and there were significant differences. Interestingly, the transplantation of hUC-MSCs apparently down-regulated the mRNA and protein expressions of Collagen I (2.11-fold and 1.40-fold), Collagen III (1.89-fold and 1.50-fold) and FGF 2 (1.77-fold and 2.0-fold) in bladder tissues induced by SCI.

Subsequently, we delved into related mechanisms. TLR4, a class of important protein molecules involved in nonspecific immunity, makes considerable impacts upon mediating chronic pain and neuroinflammation, which can be activated after

SCI [33]. The transplantation of hUC-MSCs attenuates high glucose-induced podocyte damage, and elevates intraocular pressure-induced retinal neuroinflammation via TLR4 signal [34,35]. Our results indicated that hUC-MSCs down-regulated TLR4 protein expression in bladder tissues. TLR4 has been reported to mediate the mitogen-activated protein kinase (MAPK)/NF-κB pathway [36], and MAPK is also observed to be expressed in neurons and non-neuronal cells of the mature central nervous system [37]. Besides, hUC-MSCs have been affirmed to ameliorate insulin resistance through PI3K/Akt and Erk/MAPKs signaling pathways [38]. The classic MAPK pathway (p38

MAPK), also known as stress-related protein kinase, can be strongly activated in a variety of pathological processes [39]. In SCI, apart from neurons and oligodendrocytes, the activation of p38 is observed in activated microglia/macrophages, infiltrating neutrophils and reactive astrocytes [37]. It has been reported that the activation of p38 MAPK in the bladder afferent pathway after SCI may at least partially lead to the over-excitation of C-fiber afferents through the upregulation of TRPV1, while a nonselective cation channel is mainly expressed in nociceptive primary sensory neurons [40,41], which may contribute to the possibility of some neurogenic bladder [40]. SCI resulted in the up-regulated TRPV1 (1.83-fold), TLR4 (2.18-fold), p-p38 (2.91-fold) and p-NF- κ B (1.43-fold) protein expressions in bladder tissues, while the transplantation of hUC-MSCs induced the down-regulations of TRPV1 (1.34-fold), TLR4 (1.85-fold), p-p38 (1.68-fold) and p-NF- κ B (1.25-fold) protein expressions in bladder tissues. Our research also has some limitations. For instance, we did not consider additional *in vitro* experiments to detect the NF- κ B pathway. Besides, the sample size of this study was relatively small, and only rats were used as the model subject for SCI research, which remained far from perfect. In the further researches, great efforts are required to be made on fathoming out how transplantation of hUC-MSCs into SCI rats disrupted the MAPK cascade. Apart from these, SCI tends to occur randomly in the population, with complicated pathophysiological consequences and substantial inconsistencies. However, the rat model in this study was relatively stable and simple, implying that there was a body size gap, further bringing about high degrees of uncertainty in application of hUC-MSCs on the treatment of SCI. Thus, the exploration of potential mechanism implicated in SCI still faces assorted challenges. In addition, how hUC-MSCs regulate the immune system at the injection site and systemic level may be our future research direction.

Conclusion

Nowadays, advanced interventions offer high promise for regeneration and functional restoration. Our research was in favor of the therapeutic

potential of hUC-MSCs in SCI. From the perspective of innovation, we provided the first evidence that hUC-MSCs were likely to play pivotal roles in the reconstruction of bladder functions after acute SCI through inhibiting the expressions of Collagen I, Collagen III, FGF 2, p-p38, TRPV1, TLR4 and p-NF- κ B, laying a solid foundation for their clinical application.

Authors' contributions

Substantial contributions to conception and design: Jue Li

Data acquisition, data analysis and interpretation: Jiliang Huang, Ling Chen, Wei Ren, Wenzhi Cai

Drafting the article or critically revising it for important intellectual content: Jue Li

Final approval of the version to be published: Jue Li, Jiliang Huang, Ling Chen, Wei Ren, Wenzhi Cai

Agreement to be accountable for all aspects of the work in ensuring that questions related to the accuracy or integrity of the work are appropriately investigated and resolved: Jue Li, Jiliang Huang, Ling Chen, Wei Ren, Wenzhi Cai

Availability of Data and Materials

The analyzed data sets generated during the study are available from the corresponding author on reasonable request.

Disclosure statement

No potential conflict of interest was reported by the author(s).

Funding

This work was supported by Sanming Project of Medicine in ShenZhen, China (No. SZSM201612018) and The Science and Technology Project of Shenzhen JCYJ20190814113003711JCYJ20210324142406016.

Highlight

1. HUC-MSCs restored motor function of SCI rats by ameliorating the destructive lesions.
2. HUC-MSCs ameliorated bladder dysfunction induced by SCI.
3. HUC-MSCs promoted bladder functional recovery after SCI via p38 MAPK/NF- κ B pathway.

ORCID

Wenzhi Cai  <http://orcid.org/0000-0001-8341-5479>

References

- [1] Galeiras Vazquez R, Ferreiro Velasco ME, Mourelo Farina M, et al. Update on traumatic acute spinal cord injury. Part 1. *Med Intensiva*. 2017;41:237–247.
- [2] Kjell J, Olson L. Rat models of spinal cord injury: from pathology to potential therapies. *Dis Model Mech*. 2016;9:1125–1137.
- [3] Karsy M, Hawryluk G. Modern medical management of spinal cord injury. *Curr Neurol Neurosci Rep*. 2019;19:65.
- [4] Gater DR. Neurogenic bowel and bladder evaluation strategies in spinal cord injury: new directions. *J Spinal Cord Med*. 2020;43:139–140.
- [5] Hubscher CH, Wyles J, Gallahar A, et al. Effect of different forms of activity-based recovery training on bladder, bowel, and sexual function after spinal cord injury. *Arch Phys Med Rehabil*. 2021;102:865–873.
- [6] Hu HZ, Granger N, Jeffery ND. Pathophysiology, clinical importance, and management of neurogenic lower urinary tract dysfunction caused by suprasacral spinal cord injury. *J Vet Intern Med*. 2016;30:1575–1588.
- [7] Rude T, Moghalu O, Stoffel J, et al. The role of health insurance in patient reported satisfaction with bladder management in neurogenic lower urinary tract dysfunction due to spinal cord injury. *J Urol*. 2021;205:213–218.
- [8] Romo PGB, Smith CP, Cox A, et al. Non-surgical urologic management of neurogenic bladder after spinal cord injury. *World J Urol*. 2018;36:1555–1568.
- [9] Wyndaele JJ, Birch B, Borau A, et al. Surgical management of the neurogenic bladder after spinal cord injury. *World J Urol*. 2018;36:1569–1576.
- [10] Hachem LD, Ahuja CS, Fehlings MG. Assessment and management of acute spinal cord injury: from point of injury to rehabilitation. *J Spinal Cord Med*. 2017;40:665–675.
- [11] Liao LL, Looi QH, Chia WC, et al. Treatment of spinal cord injury with mesenchymal stem cells. *Cell Biosci*. 2020;10:112.
- [12] Gao L, Peng Y, Xu W, et al. Progress in stem cell therapy for spinal cord injury. *Stem Cells Int*. 2020;2020:2853650.
- [13] Ahuja CS, Mothe A, Khazaei M, et al. The leading edge: emerging neuroprotective and neuroregenerative cell-based therapies for spinal cord injury. *Stem Cells Transl Med*. 2020;9:1509–1530.
- [14] Deng WS, Ma K, Liang B, et al. Collagen scaffold combined with human umbilical cord-mesenchymal stem cells transplantation for acute complete spinal cord injury. *Neural Regen Res*. 2020;15:1686–1700.
- [15] Xiao Z, Tang F, Zhao Y, et al. Significant improvement of acute complete spinal cord injury patients diagnosed by a combined criteria implanted with neuroregen scaffolds and mesenchymal stem cells. *Cell Transplant*. 2018;27:907–915.
- [16] Xie Q, Liu R, Jiang J, et al. What is the impact of human umbilical cord mesenchymal stem cell transplantation on clinical treatment? *Stem Cell Res Ther*. 2020;11:519.
- [17] Yamazaki K, Kawabori M, Seki T, et al. FTY720 attenuates neuropathic pain after spinal cord injury by decreasing systemic and local inflammation in a rat spinal cord compression model. *J Neurotrauma*. 2020;37:1720–1728.
- [18] Zhang L, Zhuang X, Chen Y, et al. Intravenous transplantation of olfactory bulb ensheathing cells for a spinal cord hemisection injury rat model. *Cell Transplant*. 2019;28:1585–1602.
- [19] Munoz A, Yazdi IK, Tang X, et al. Localized inhibition of P2X7R at the spinal cord injury site improves neurogenic bladder dysfunction by decreasing urothelial P2X3R expression in rats. *Life Sci*. 2017;171:60–67.
- [20] Sun L, Wang F, Chen H, et al. Co-transplantation of human umbilical cord mesenchymal stem cells and human neural stem cells improves the outcome in rats with spinal cord injury. *Cell Transplant*. 2019;28:893–906.
- [21] Basso DM, Beattie MS, Bresnahan JC. A sensitive and reliable locomotor rating scale for open field testing in rats. *J Neurotrauma*. 1995;12:1–21.
- [22] Basso DM, Beattie MS, Bresnahan JC, et al. MASCIS evaluation of open field locomotor scores: effects of experience and teamwork on reliability. *Multicenter Animal Spinal Cord Injury Study*. *J Neurotrauma*. 1996;13:343–359.
- [23] Bao CS, Li XL, Liu L, et al. Transplantation of Human umbilical cord mesenchymal stem cells promotes functional recovery after spinal cord injury by blocking the expression of IL-7. *Eur Rev Med Pharmacol Sci*. 2018;22:6436–6447.
- [24] Fan B, Wei Z, Yao X, et al. Microenvironment imbalance of spinal cord injury. *Cell Transplant*. 2018;27:853–866.
- [25] Salehi-Pourmehr H, Hajebrahami S, Rahbarghazi R, et al. Stem cell therapy for neurogenic bladder dysfunction in rodent models: a systematic review. *Int Neurourol J*. 2020;24:241–257.
- [26] Yang Y, Cao TT, Tian ZM, et al. Subarachnoid transplantation of human umbilical cord mesenchymal stem cell in rodent model with subacute incomplete spinal cord injury: preclinical safety and efficacy study. *Exp Cell Res*. 2020;395:112184.
- [27] Li X, Tan J, Xiao Z, et al. Transplantation of hUC-MSCs seeded collagen scaffolds reduces scar formation and promotes functional recovery in canines with chronic spinal cord injury. *Sci Rep*. 2017;7:43559.
- [28] Wu LL, Pan XM, Chen HH, et al. Repairing and analgesic effects of umbilical cord mesenchymal stem cell transplantation in mice with spinal cord injury. *Biomed Res Int*. 2020;2020:7650354.

- [29] Yang Y, Pang M, Du C, et al. Repeated subarachnoid administrations of allogeneic human umbilical cord mesenchymal stem cells for spinal cord injury: a phase 1/2 pilot study. *Cytotherapy*. 2021;23:57–64.
- [30] Fowler CJ, Griffiths D, de Groat WC. The neural control of micturition. *Nat Rev Neurosci*. 2008;9:453–466.
- [31] WenBo W, Fei Z, YiHeng D, et al. Human umbilical cord mesenchymal stem cells overexpressing nerve growth factor ameliorate diabetic cystopathy in rats. *Neurochem Res*. 2017;42:3537–3547.
- [32] Shunmugavel A, Khan M, Hughes FM Jr., et al. S-Nitrosoglutathione protects the spinal bladder: novel therapeutic approach to post-spinal cord injury bladder remodeling. *Neurourol Urodyn*. 2015;34:519–526.
- [33] Xu S, Wang J, Jiang J, et al. TLR4 promotes microglial pyroptosis via lncRNA-F630028O10Rik by activating PI3K/AKT pathway after spinal cord injury. *Cell Death Dis*. 2020;11:693.
- [34] Ji S, Xiao J, Liu J, et al. Human umbilical cord mesenchymal stem cells attenuate ocular hypertension-induced retinal neuroinflammation via toll-like receptor 4 pathway. *Stem Cells Int*. 2019;2019:9274585.
- [35] Wang Y, Liu J, Zhang Q, et al. Human umbilical cord mesenchymal stem cells attenuate podocyte injury under high glucose via TLR2 and TLR4 signaling. *Diabetes Res Clin Pract*. 2021;173:108702.
- [36] Zhou J, Liu Q, Qian R, et al. Paeonol antagonizes oncogenesis of osteosarcoma by inhibiting the function of TLR4/MAPK/NF-kappaB pathway. *Acta Histochem*. 2020;122:151455.
- [37] Falcicchia C, Tozzi F, Arancio O, et al. Involvement of p38 MAPK in synaptic function and dysfunction. *Int J Mol Sci*. 2020;21(16):5624.
- [38] Chen G, Fan XY, Zheng XP, et al. Human umbilical cord-derived mesenchymal stem cells ameliorate insulin resistance via PTEN-mediated crosstalk between the PI3K/Akt and Erk/MAPKs signaling pathways in the skeletal muscles of db/db mice. *Stem Cell Res Ther*. 2020;11:401.
- [39] Kasuya Y, Umezawa H, Hatano M. Stress-activated protein kinases in spinal cord injury: focus on roles of p38. *Int J Mol Sci*. 2018;19(3):867.
- [40] Shimizu N, Wada N, Shimizu T, et al. Role of p38 MAP kinase signaling pathways in storage and voiding dysfunction in mice with spinal cord injury. *Neurourol Urodyn*. 2020;39:108–115.
- [41] Caterina MJ, Julius D. The vanilloid receptor: a molecular gateway to the pain pathway. *Annu Rev Neurosci*. 2001;24:487–517.